Influence of charge asymmetry and isospin-dependent cross section on nuclear stopping

Anupriya Jain and Suneel Kumar*
School of Physics and Material Science, Thapar University, Patiala-147004, Punjab, India

Rajeev K. Puri
Department of Physics, Panjab University, Chandigarh-160014, India
(Received 15 September 2011; published 21 November 2011)

Using the isospin-dependent quantum molecular dynamics model, we study the effect of charge asymmetry and isospin-dependent cross section on nuclear stopping and multiplicity of free nucleons and light mass fragments. Simulations were carried out for the reactions $^{124}X_m + {}^{124}X_m$, where m varies from 47 to 59 and for $^{40}Y_n + {}^{40}Y_n$, where n varies from 14 to 23. Our study shows that nuclear stopping depends strongly on the isospin of the cross section.

DOI: 10.1103/PhysRevC.84.057602 PACS number(s): 25.70.Pq, 21.65.Ef

Heavy-ion collisions (HICs) provide a unique opportunity to produce a small amount of nuclear matter with high density and high temperature in a controlled fashion. By measuring the final products of the collisions, it is possible to learn about the fundamental properties of the hot and compressed nuclear matter, namely, the nuclear equation of state (EOS) [1–3]. To link the experimental observations and EOS extracted from the HICs, we need a transport model where nucleon-nucleon two-body collisions and mean-field effects are carefully treated [4–6].

One of the key observables in HICs is the nuclear stopping that can be studied with the help of the rapidity distribution [7] and the asymmetry of the nucleon momentum distribution [8]. Bauer [9] pointed out that nuclear stopping power in intermediate energy HIC is determined by both mean field as well as in-medium nucleon-nucleon cross-section. It is worth mentioning that symmetry potential was not included in their analysis. Peilert *et al.* [10] suggested that the degree of approaching isospin equilibration provides a mean to probe the mechanism and power of the nuclear stopping in HICs.

Fu *et al.* [11] calculated both the radial flow and the degree of nuclear stopping using the reactions of Pb + Pb and Ni + Ni at 0.4, 0.8, and 1.2 GeV/nucleon. They found that the expansion velocity as well as the degree of nuclear stopping are higher in a heavier system irrespective of the incident energies.

Li and Li [12] studied the dependence of nuclear stopping $\langle Q_{ZZ}/A\rangle$ and $\langle R\rangle$ in intermediate-energy HICs on system size, initial N/Z, isospin symmetry potential, and medium corrections of two-body cross sections. They showed that the effect of the initial N/Z ratio, as well as isospin symmetry potential, is weak on stopping. The excitation function of $\langle Q_{ZZ}/A\rangle$ and $\langle R\rangle$, however, depends on the form of the medium corrections of two-body cross sections and on the EOS of nuclear matter. Moreover, they showed that the behavior of excitation function of $\langle Q_{ZZ}/A\rangle$ and R can provide clearer information about the isospin dependence of the medium correction of two-body cross sections.

Liu *et al.* [13] studied the nuclear stopping for various colliding systems with different neutron-proton ratios over large domains of incident energy. Nuclear stopping was found to be very sensitive toward the isospin content of in-medium nucleon-nucleon cross section above Fermi energy. The results were, however, insensitive toward the symmetry potential. They proposed that nuclear stopping can be used as a new probe to extract the information about the isospin dependence of the in-medium nucleon-nucleon cross section in intermediate-energy HICs. However, Li *et al.* [14] showed that traditional measures of the nuclear stopping power are found to be sensitive to the magnitude of the in-medium nucleon-nucleon cross sections but they are ambiguous for determining the isospin dependence of the in-medium nucleon-nucleon cross sections. In this study, our aim is to pin down the influence of charge asymmetry, as well as different cross sections [$\sigma_{\rm iso}$ (isospin dependent) and $\sigma_{\rm noiso}$ (isospin independent)] [15,16], on nuclear stopping observables such as $\langle R\rangle$, $\langle 1/Q_{ZZ}\rangle$, and multiplicity of free nucleons and light mass fragments (LMFs).

Our study is performed within the framework of the isospin-dependent quantum molecular dynamics [5,16] model, where hadrons propagate with Hamilton equations of motion:

$$\frac{dr_i}{dt} = \frac{d\langle H\rangle}{dp_i}; \quad \frac{dp_i}{dt} = -\frac{d\langle H\rangle}{dr_i}, \tag{1}$$

with

$$\begin{aligned}\langle H\rangle &= \langle T\rangle + \langle V\rangle \\ &= \sum_i \frac{p_i^2}{2m_i} + \sum_i \sum_{j>i} \int f_i(\vec{r},\vec{p},t) V^{ij}(\vec{r}\,',\vec{r}) \\ &\quad \times f_j(\vec{r}\,',\vec{p}\,',t) d\vec{r} d\vec{r}\,' d\vec{p} d\vec{p}\,'. \end{aligned} \tag{2}$$

The baryon-baryon potential V^{ij}, in the above relation, reads as

$$\begin{aligned} V^{ij}(\vec{r}\,'-\vec{r}) &= V^{ij}_{\rm Skyrme} + V^{ij}_{\rm Yukawa} + V^{ij}_{\rm Coul} + V^{ij}_{\rm sym} \\ &= \left[t_1 \delta(\vec{r}\,'-\vec{r}) + t_2 \delta(\vec{r}\,'-\vec{r}) \rho^{\gamma-1}\left(\frac{\vec{r}\,'+\vec{r}}{2}\right)\right] \\ &\quad + t_3 \frac{exp(|\vec{r}\,'-\vec{r}|/\mu)}{(|\vec{r}\,'-\vec{r}|/\mu)} + \frac{Z_i Z_j e^2}{|\vec{r}\,'-\vec{r}|} \\ &\quad + t_6 \frac{1}{\varrho_0} T_3^i T_3^j \delta(\vec{r}_i\,'-\vec{r}_j). \end{aligned} \tag{3}$$

*suneel.kumar@thapar.edu

 ©2011 American Physical Society

Here Z_i and Z_j denote the charges of ith and jth baryon, and T_3^i, T_3^j are their respective T_3 components (i.e., 1/2 for protons and −1/2 for neutrons). Meson potential consists of Coulomb interaction only. The parameters μ and $t_1, \ldots, t_6$ are adjusted to the real part of the nucleonic optical potential.

The binary nucleon-nucleon collisions are included by employing the collision term of the well-known Vlasoz-Uehling-Uhlenbeck–Boltzmann-Uehling-Uhlenback equation. During the propagation, two nucleons are supposed to suffer a binary collision if the distance between their centroids,

$$|r_i - r_j| \leqslant \sqrt{\frac{\sigma_{\rm tot}}{\pi}}, \quad \sigma_{\rm tot} = \sigma(\sqrt{s}, \text{type}), \tag{4}$$

where "type" denotes the ingoing collision partners (N-N, N-Δ, N-π, ...). In addition, Pauli blocking (of the final state) of baryons is taken into account by checking the phase space densities in the final states.

Nuclear stopping is investigated using three observables. The first one is anisotropy ratio $\langle R\rangle$ [13,16], defined as

$$\langle R\rangle = \frac{2}{\pi}\frac{\left[\sum_i p_\perp(i)\right]}{\left[\sum_i p_\parallel(i)\right]}, \tag{5}$$

where $p_\perp(i) = \sqrt{(p_x^2(i) + p_y^2(i))}$ and $p_\parallel(i) = p_Z(i)$, respectively. If $\langle R\rangle = 1$, then it means complete stopping.

Second parameter is the quadrupole moment $\langle Q_{ZZ}\rangle$ [13,16], defined as

$$\langle Q_{ZZ}\rangle = \sum_i 2p_z^2(i) - p_x^2(i) - p_y^2(i). \tag{6}$$

For complete stopping $\langle Q_{ZZ}\rangle = 0$.

The third parameter is rapidity distribution $Y(i)$ [16,17], defined as

$$Y(i) = \frac{1}{2}\ln\frac{E(i) + p_z(i)}{E(i) - p_z(i)}, \tag{7}$$

where, $E(i)$ and $p_Z(i)$ are the total energy and longitudinal momentum, respectively.

For the present analysis, simulations are carried out for two sets of reactions using soft EOS. For the first case, mass of the colliding nuclei is fixed to be 40 units, but charge varies from 14 to 23. In other words, we study $^{40}X_m + {}^{40}X_m$, where $^{40}X_m = ({}^{40}V_{23}, {}^{40}Sc_{21}, {}^{40}Ca_{20}, {}^{40}Ar_{18}, {}^{40}Cl_{17}, {}^{40}S_{16}, {}^{40}P_{15}$, and $^{40}Si_{14})$, respectively. For the second set, we have chosen those reactions where the mass of the each colliding nuclei is fixed to be 124 units, but charge varies from 47 to 59. The second set of the reactions taken are $^{124}Y_n + {}^{124}Y_n$, where $^{124}Y_n = ({}^{124}Ag_{47}, {}^{124}Cd_{48}, {}^{124}In_{49}, {}^{124}Sn_{50}, {}^{124}I_{53}, {}^{124}Cs_{55}, {}^{124}Ba_{56}$, and $^{124}Pr_{59})$, respectively. Figure 1 shows the rapidity distribution $\langle dN/dY\rangle$ for the emission of free nucleons (FNs) ($A = 1$) and LMFs ($2 \leqslant A \leqslant 4$) at an incident energy of $E = 100$ MeV/nucleon. To check the role of different cross sections on the rapidity distribution, two reactions $^{124}Ag_{47} + {}^{124}Ag_{47}$ and $^{124}Pr_{59} + {}^{124}Pr_{59}$ are displayed. This choice of reaction panels throws light on the role of charge asymmetry. As noted by many authors, FNs and LMFs are produced from the participant zone, whereas intermediate mass fragments (IMFs) ($5 \leqslant A \leqslant A_{\rm tot}/6$) are mostly produced out of the spectator matter.

We also noted clear isospin effects on the production of free nucleons and LMFs in the energy region of midrapidity.

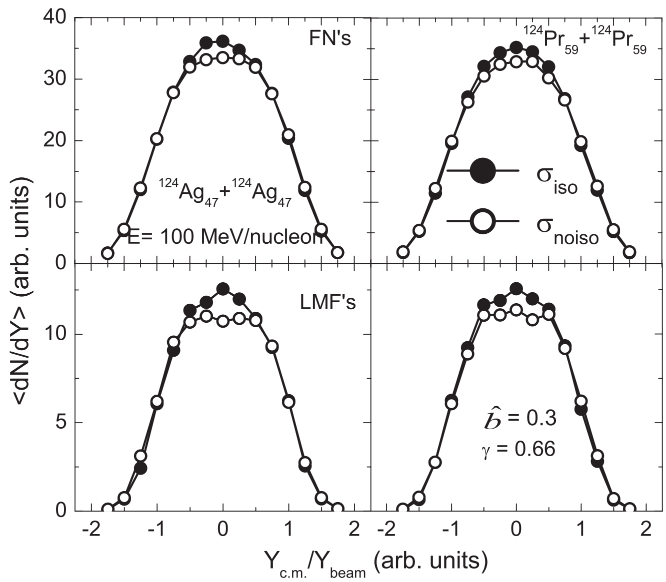

FIG. 1. Rapidity distribution of FNs and LMFs.

This happens owing to the fact that $\sigma_{\rm iso}$ [near midrapidity $(-0.1 < \frac{Y_{\rm c.m.}}{Y_{\rm beam}} < 0.1)$] will enhance the binary collisions that results in enhanced production. This effect should diminish as we move away from the midrapidity region, where either a targetlike or a projectilelike process dominates.

Strikingly, very little influence (less than 3%) is noted owing to charge asymmetry. Note that while mass remains fixed, charge of the colliding nuclei varies from 47 to 59 units. To check the effect of isospin dependence of cross-section on nuclear stopping, we display in Fig. 2 the impact parameter dependence of the stopping observables ($\langle R\rangle$ and $\langle 1/Q_{ZZ}\rangle$). The results are displayed at 100 MeV/nucleon for the reactions of $^{40}Si_{14} + {}^{40}Si_{14}$, $^{40}V_{23} + {}^{40}V_{23}$, $^{124}Ag_{47} + {}^{124}Ag_{47}$, and $^{124}Pr_{59} + {}^{124}Pr_{59}$. We observe the following.

(1) $\langle R\rangle$ and $\langle 1/Q_{ZZ}\rangle$ behave in a similar fashion. The amount of stopping decreases with the impact parameter. Reduced participant matter is the cause for this decrease.

(2) The value of the stopping is more for $\sigma_{\rm iso}$ than for $\sigma_{\rm noiso}$ (8% in the case of $\langle R\rangle$ and 26% in the case of $\langle 1/Q_{ZZ}\rangle$). This happens because isospin-dependent cross section will lead to violent NN collisions that will further cause the transformation of the initial longitudinal motion in other directions and hence thermalization of the system. This dominant role played by the isospin-dependent cross-section gradually disappears with the impact parameter. These findings are also in supportive nature with the findings of Ref. [13].

(3) On comparing the value of stopping for both the reacting series, $^{124}Ag_{47} + {}^{124}Ag_{47}$, $^{124}Pr_{59} + {}^{124}Pr_{59}$, $^{40}Si_{14} + {}^{40}Si_{14}$, and $^{40}V_{23} + {}^{40}V_{23}$, we found that heavier masses lead to better thermalization compared to lighter nuclei.

As noted in the Refs. [13,17,18], the production of free nucleons and LMFs behave in similar fashion as $\langle R\rangle$ and $\langle 1/Q_{ZZ}\rangle$. To check the effect of charge asymmetry on the

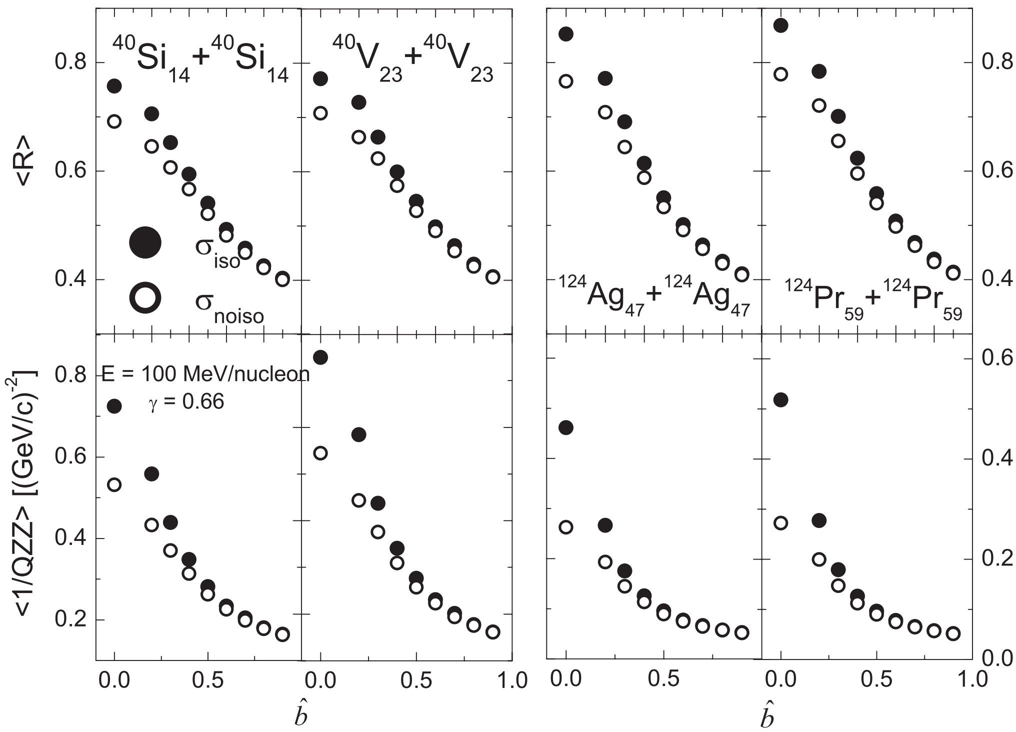

FIG. 2. Variation of $\langle R \rangle$ and $\langle 1/Q_{ZZ} \rangle$ as a function of $\hat{b}$.

nuclear stopping parameters, we display in Fig. 3 the variation of stopping parameters as a function of Z for two different cross sections $\sigma_{\rm iso}$ and $\sigma_{\rm noiso}$ for both series of reactions. In the left panels, we use $^{40}X_m + {}^{40}X_m$ (where m varies from 14 to 23), whereas in the right panels we use $^{124}Y_n + {}^{124}Y_n$ (where n varies from 47 to 59). We note that $\langle R \rangle$ and $\langle 1/Q_{ZZ} \rangle$ behave in a similar way. Further, very weak dependence is visible for charge asymmetry. This result is similar as reported in earlier figures. This observation is in agreement with the observation in Ref. [17].

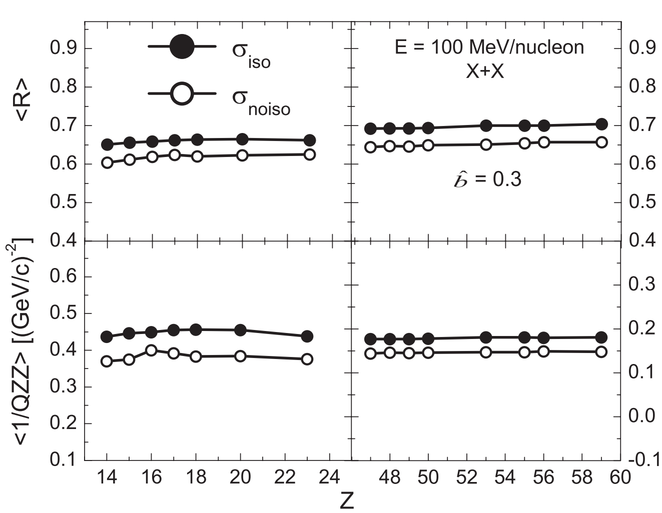

FIG. 3. Variation of $\langle R \rangle$ and $\langle 1/Q_{ZZ} \rangle$ with Z: in left panel for $X = {}^{40}V_{23}, {}^{40}Sc_{21}, {}^{40}Ca_{20}, {}^{40}Ar_{18}, {}^{40}Cl_{17}, {}^{40}S_{16}, {}^{40}P_{15}, {}^{40}Si_{14}$ and in right panel for $X = {}^{124}Ag_{47}, {}^{124}Cd_{48}, {}^{124}In_{49}, {}^{124}Sn_{50}, {}^{124}I_{53}, {}^{124}Cs_{55}, {}^{124}Ba_{56}, {}^{124}Pr_{59}$.

To further strengthen our interpretation of the results, in Fig. 4 we display the comparison of theoretical results of anisotropy ratio with the experimental data obtained by the INDRA collaboration [19]. Here simulations are performed for the reaction $^{124}Sn_{50} + {}^{124}Sn_{50}$ with $\sigma_{\rm iso}$ reduced by 20%. It is worth mentioning that the results with the above choice of cross section are in good agreement with the experimental data of Ref. [19]. The choice of reduced cross section has also been motivated by Ref. [20] as well as many previous studies [21]. From Fig. 4 we also note that anisotropy ratio decreases with increase in the incident energy. This happens because transverse components associated with the nucleons decreases with incident energy. These findings are in agreement with the studies recorded in Ref. [13].

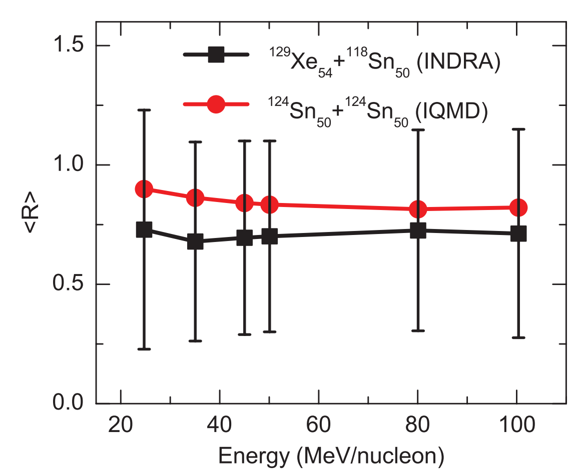

FIG. 4. (Color online) The anisotropy ratio $\langle R \rangle$ as a function of beam energy.

By using the isospin-dependent quantum molecular dynamics model, we have studied the effect of charge asymmetry and isospin-dependent cross section on nuclear stopping and multiplicity of free nucleons and LMFs. The calculations were carried out for $^{124}X_m + {}^{124}X_m$, where m varies from 47 to 59 and for $^{40}Y_n + {}^{40}Y_n$, where n varies from 14 to 23. Nuclear stopping was found to depend strongly on the isospin-dependent cross section. Moreover, theoretical results on the anisotropy ratio $\langle R \rangle$ follow the same trend as recorded by INDRA collaboration.

This work has been supported by a grant from the university grant commission, Government of India [Grant No. 39-858/ 2010(SR)].

[1] H. Stöcker and W. Greiner, Phys. Rep. **137**, 277 (1986).
[2] P. Danielewicz, R. Lacey, and W. G. Lynch, Science **298**, 1592 (2002).
[3] T. Klahn *et al.*, Phys. Rev. C **74**, 035802 (2006).
[4] J. Aichelin, Phys. Rep. **202**, 233 (1991).
[5] C. Hartnack *et al.*, Eur. Phys. J. A **1**, 151 (1998).
[6] E. E. Kolomeitsev *et al.*, J. Phys. G **31**, s741 (2005).
[7] C. Y. Wong, *Introduction to High-Energy Heavy-Ion Collisions* (World Scientific, Singapore, 1994).
[8] B. A. Li and C. M. Ko, Nucl. Phys. A **601**, 457 (1996).
[9] W. Bauer, Phys. Rev. Lett. **61**, 2534 (1988).
[10] G. Peilert, H. Stocker, W. Greiner, A. Rosenhauer, A. Bohnet, and J. Aichelin, Phys. Rev. C **39**, 1402 (1989).
[11] F. Fu *et al.*, Phys. Lett. B **666**, 359 (2008).
[12] Q. Li and Z. Li, Chin. Phys. Lett. **19**, 321 (2002).
[13] J. Y. Liu, W. J. Guo, S. J. Wang, W. Zuo, Q. Zhao, and Y. F. Yang, Phys. Rev. Lett. **86**, 975 (2001).
[14] B.-A. Li, P. Danielewicz, and W. G. Lynch, Phys. Rev. C **71**, 054603 (2005).
[15] T. Izumoto, S. Krewald, and A. Faessler, Nucl. Phys. A **341**, 319 (1980); A. Faessler and W. H. Dickhoff, *ibid.* **428**, 271c (1981); M. Trefz, A. Faessler, and W. H. Dickhoff, *ibid.* **443**, 499 (1985); N. Ohtsuka, R. Linden, A. Faessler, and F. B. Malik, *ibid.* **465**, 550 (1987).
[16] J. Aichelin, Phys. Rep. **202**, 233 (1991); R. K. Puri *et al.*, Nucl. Phys. A **575**, 733 (1994); E. Lehmann, R. K. Puri, A. Faessler, G. Batko, and S. W. Huang, Phys. Rev. C **51**, 2113 (1995); Y. K. Vermani *et al.*, J. Phys. G: Nucl. Part. Phys. **36**, 105103 (2009); **37**, 015105 (2010); Y. K. Vermani, S. Goyal, and R. K. Puri, Phys. Rev. C **79**, 064613 (2009); S. Kumar, S. Kumar, and R. K. Puri, *ibid.* **81**, 014601 (2010).
[17] T. Gaitanos *et al.*, Phys. Lett. B **595**, 209 (2004); M. Di Toro *et al.*, Nucl. Phys. A **787**, 585 (2007).
[18] S. Kumar, S. Kumar, and R. K. Puri, Phys. Rev. C **81**, 014611 (2010); V. Kaur, S. Kumar, and R. K. Puri, Phys. Lett. B **697**, 512 (2011).
[19] G. Lehaut *et al.*, Phys. Rev. Lett. **104**, 232701 (2010).
[20] S. Gautam and A. D. Sood, Phys. Rev. C **82**, 014604 (2010).
[21] F. Daffin and W. Bauer, arXiv:nucl-th/9809024v1.